J. MACROMOL. SCI.—PHYS., B39(5&6), 711–722 (2000)

The Nonisothermal Crystallization Kinetics of Polypropylene After DSC Calibration on Cooling

J. A. MARTINS[1,*] and J. J. C. CRUZ PINTO[2]
[1]Departamento de Engenharia de Polímeros
Universidade do Minho
Campus de Azurém
4800-058 Guimarães, Portugal
[2]Departamento de Química
Universidade de Aveiro
3810-193, Aveiro, Portugal

ABSTRACT

The effect of the temperature scale on the nonisothermal crystallization of a polypropylene (PP) was studied with the Nakamura equation and a Tobin-type equation for nonisothermal crystallization. The calibration on cooling of differential scanning calorimetry (DSC) data was performed, and the scanning rate dependence of the sample's thermal resistance was evaluated and taken into account to correct the nonisothermal crystallization data obtained from the DSC measurements. The description of the crystallization was performed with only one varying parameter, which changed regularly with the scanning rate, making possible predictions of real nonisothermal crystallization behavior at intermediate or high scanning rates.

Key Words. Calibration, Cooling, Crystallization, Kinetics, Nonisothermal.

*To whom correspondence should be addressed. E-mail: zmartins@eng.uminho.pt

INTRODUCTION

The properties of plastic components are affected greatly by their processing conditions. In the processing of semicrystalline polymers, the crystallization may take more than half of the production cycle time, determining the final degree of crystallinity and morphology. It is well known the importance played by these two parameters on the final product properties. They are affected not only by the shear and elongational flows, but also by the thermal gradients within the sample, which are greatly dependent on the cooling rate of the melt. Only a quantitative description of the nonisothermal crystallization kinetics of polymer melts may provide appropriate information concerning the supercooling and the temperature range of crystallization.

The nonisothermal crystallization kinetics of polymers usually are described by the Nakamura equation [1]. Although Nakamura claims the validity of his equation to nonisothermal crystallization processes with both primary instantaneous and sporadic nucleations, it was recently shown that the validity is restricted only to processes with primary instantaneous (or athermal) nucleation [2]. The isokinetic condition, used by Nakamura in the derivation of his equation, is an artificial way to extend the Avrami equation to nonisothermal crystallization with sporadic nucleation. This condition assumes that the primary nucleation, governed by the activation frequency of the primary nuclei (or probability of occurrence of an activation per unit time), shows the same time dependence (or temperature dependence) as the secondary nucleation. In this way, the ratio between the linear growth rate of the spherulites and the activation frequency of the primary nuclei is assumed to be constant [1]. The validity of the isokinetic assumption, however, is limited to a narrow temperature range or, in an isothermal crystallization process, to the initial times.

Equations of Avrami type, either for instantaneous or sporadic nucleation, may be derived without assuming the isokinetic condition [2,3]. The equation then obtained for instantaneous nucleation is the Nakamura equation [2], briefly outlined below. Similarly, a Tobin-type nonisothermal equation is also derived below.

Both equations can be used to describe nonisothermal crystallization using only two adjustable parameters: the exponent n and a preexponential factor. Values of the other parameters used in those equations may be set to the values obtained from isothermal experiments, either from the half-crystallization times or the spherulite radial growth rates.

Despite the theoretical and experimental work done in this field, a precise description of nonisothermal crystallization of quiescent polymer melts is yet to be achieved. One of the problems is whether use should be made of parameters determined from isothermal experiments, namely, those related to the temperature dependence of the linear growth rate, to model nonisothermal crystallization kinetics. From a physical point of view, the temperature dependence of the linear growth rate of the spherulites is independent of the nature of the crystallization process, and so use should be made of the more accurate information obtainable from isothermal experiments. Often, however, when this procedure is used, the resulting parameter values are physically unacceptable. Ways of dealing with the problem include considering/using freely changing parameters, arbitrarily defined (and thus physically unjustifiable) induction times, physically incorrect equations [4], equations with an excessive number of parameters (often with no physical meaning), or arbitrary combinations of single-mechanism equations [5].

Indeed, two reasons may be identified for failing to describe nonisothermal crystallization with a reduced set of parameters. The first is the inadequacy of the theoretical

MARCEL DEKKER, INC.
270 Madison Avenue, New York, New York 10016

models, and the second is a wrong sample temperature assignment during the crystallization process. Concerning this last factor, it may be easily corrected by proper temperature calibration (calibration on cooling) and by accounting for the effect of the sample's thermal resistance on the true sample temperature [6]. Ways to deal with this last effect have been referred to in the literature [6,7].

Concerning the calibration on cooling, a common and accepted way to implement it is to use isotropic-to-nematic (I → N) liquid crystal transitions [8]. An alternative way involves the use of the melting onsets of the same high-purity metal standards used to perform the calibration on heating to also calibrate on cooling by an adequate, physically well-based, procedure [6], a summary of which is also presented below. The errors involved in using the proposed method are similar in magnitude to the errors obtained when liquid crystalline transitions are used.

NONISOTHERMAL CRYSTALLIZATION

The Nakamura Equation—An Alternative Derivation

The derivation of the Nakamura equation is valid only for instantaneous nucleation. According to the definition of Wunderlich, this nucleation, also called athermal, implies that all crystals start growing at the same time and temperature (during cooling) [9].

For freely growing spheres, the mass fraction transformed between t and $t + dt(dX')$ is given by

$$dX' = \frac{\rho_s}{\rho_l} \overline{N}\, 4\pi r^2 dr \tag{1}$$

where r is the radius at time t, $\overline{N}$ is the mean number of growing nuclei existing in a unit volume of untransformed material, and ρ_s and ρ_l are the solid and liquid phase densities, respectively.

Equation 1 may be expressed as a function of temperature and cooling rate as

$$dX' = \frac{\rho_s}{\rho_l} \overline{N} 4\pi r^2 G dt = \frac{\rho_s}{\rho_l} \overline{N} 4\pi r^2 G \frac{dt}{dT} dT \tag{2}$$

where G is the linear growth rate of the spheres, and $\dot{T} = dT/dt$ is the scanning rate (usually constant), which, for a cooling experiment, is negative. After accounting for the effect of spherulite impingement, according to Avrami, we have

$$\int_o^x \frac{dX}{1-X} = \frac{4\pi\rho_s \overline{N}}{\rho_l} \int_{T_m^0}^{T} \frac{r^2 G(T')}{\dot{T}} dT' \tag{3}$$

where T_m^0 is the thermodynamic melting temperature.

The integral in the right-hand side of Eq. 3 may be solved by parts, to give $r^3(t)/3$. Since

$$r(t) = \int_o^t G(T)dt = \int_{T_m^0}^{T} G(T') \frac{1}{\dot{T}} dT' = \frac{T - T_m^0}{\dot{T}} \overline{G}(T) \tag{4}$$

where the last equality applies only for constant scanning rate, the solution of Eq. 3 is the Nakamura equation,

$$X(T) = 1 - \exp\left\{ -\left[\int_{T_m^0}^{T} Z(T') \frac{1}{\dot{T}} dT' \right]^3 \right\} \tag{5}$$

with

$$Z(T) = \left\{ \frac{4\pi\rho_s \overline{N}}{3\rho_l \dot{T}^3} [G(T)]^3 \right\}^{1/3} \tag{6}$$

When Eq. 5 is used to describe the nonisothermal crystallization kinetics under a specified constant cooling rate, two parameters are allowed to change: the exponent n (in the above case, 3) and a preexponential factor, which includes the shape factor for a sphere, the mean number of primary nuclei, the ratio of the densities, and the preexponential factor of the linear growth rate equation. The other parameters in the expression of the linear growth rate may be assigned the values obtained from isothermal crystallization experiments.

A Tobin-Type Nonisothermal Equation

Using reasoning similar to that used above, a Tobin-type nonisothermal equation may also be derived. The only difference is the manner used to account for the impingement between the crystalline growing structures. According to Tobin, the impingement is accounted for by

$$X(t) = [1 - X(t)] \cdot X'(t) \tag{7}$$

where $X'(t)$ is the mass fraction transformed for freely growing spheres, which is given by

$$X'(t) = \frac{4\pi\rho_s \overline{N}}{\rho_l} \int_{T_m^0}^{T} \frac{r^2 G(T')}{\dot{T}} dT' \tag{8}$$

Using the result of the solution of the right-hand side integral and Eq. 4, Eq. 7 yields

$$\frac{X(T)}{1 - X(T)} = \left[\int_{T_m^0}^{T} Z(T') \frac{1}{\dot{T}} dT' \right]^3 \tag{9}$$

with $Z(T)$ also given by Eq. 6.

Calibration on Cooling

When a differential scanning calorimeter (DSC) is calibrated for a heating experiment, two corrections are performed automatically: an isothermal correction, for the sensor temperature reading in the limit of zero scanning rate, and a scanning rate correction, which increases with the scanning rate in use and includes the effect of the thermal resistances of the sample holder (oven and sensors), the aluminum pan, and the standard metal. The calibration line including the above effects is

$$T_t^+ = a^+ T_m + b^+ \tag{10}$$

where T_m is the measured temperature, which only equals the true sensor temperature when no isothermal correction is needed (i.e., when the temperature sensor is calibrated automatically for isothermal experiments) [6]. For other situations, the isothermal correction must be calculated, for example, by extrapolation to the zero scanning rate of the melting onsets of standard, very pure, materials, like indium and lead. The isothermal correction is then

$$\Delta T_0 = T_m - T_{sh} \tag{11}$$

where T_{sh} is the true temperature of the sample holder. The constants a^+ and b^+ correct for the scanning rate–dependent thermal lag.

When samples of different mass and heat capacity (for example, polymer samples) are used, the effect of the sample's thermal resistance must be accounted for by

$$T_t^+ = a^+ T_m + b^+ - R_s \Delta \dot{Q}^+ \tag{12}$$

where $\Delta \dot{Q}^+$ is the difference of heat fluxes crossing the sample and reference ovens with baseline correction, and R_s is the difference between the thermal resistances of the sample and the calibrant.

To calibrate a DSC on cooling from the melting onsets of standard metals, we only need to consider the correction for the real, actually acting, thermal lag due to the negative scanning rate. According to the working principle of a DSC, for a given heat flux and cell resistance, the thermal lag on cooling is simply symmetrical to that on heating, that is,

$$\Delta T^- = -\Delta T^+ \Leftrightarrow (T_t^- - T_{sh}) = -(T_t^+ - T_{sh}) \tag{13}$$

which may be expressed as

$$T_t^- = 2T_{sh} - T_t^+ \tag{14}$$

After substituting Eq. 10 in Eq. 14 and using the definition of the isothermal correction given by Eq. 11, we have

$$T_t^- = (2 - a^+) T_m - b^- \tag{15}$$

with $b^- = 2\Delta T_0 + b^+$. This equation allows us to correct the measured temperatures during a cooling scan, without any additional calibration, providing that the melting onsets of two standards and the isothermal correction are known. It must be noticed that Eq. 15 corrects the measured temperatures on cooling for both the thermal lag due to the scanning rate and the constant thermal lag due to the isothermal correction [6]. Further corrections needed in Eq. 15 are, according to Eq. 12, the thermal lag due to the sample's thermal resistance and the possible variation of the isothermal correction in the temperature range of interest [6]. Considering a linear variation of the isothermal correction in the temperature range of interest, this last correction can easily be performed. Similar to the heating case, the effect of the sample's thermal resistance can now (in cooling) be accounted for by

$$T_t^- = (2 - a^+) T_m - b^- + R_s |\Delta \dot{Q}^-| \tag{16}$$

Both Eq. 12 and Eq. 15 are, however, only approximate, being strictly applicable only for not too fast and highly exothermal or endothermal processes. More exact (ordinary differential) equations may be found in Ref. 2.

MARCEL DEKKER, INC.
270 Madison Avenue, New York, New York 10016

EXPERIMENTAL

A Perkin-Elmer DSC7 (Norwalk, CT) was used in this work. A liquid crystal, reference CBOOA [*N*-(4-octyloxyphenyl)-4-cyanobenzaldimine] (Merck, Hoddesdon, UK) was used to check the calibration on cooling. Its chemical structure is

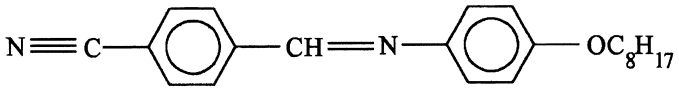

and, according to the manufacturer, the phase diagram is

$$K\ -78.8\ -S_A\ -83.0\ -N\ -107.0\ -I$$

where K = crystal, S_A = smectic, N = nematic, and I = isotropic.

A sample with a mass of 5.029 mg was placed in an aluminum pan identical to that used for the indium sample. The purity of this liquid crystal, as measured by DSC, was 99.985%.

Several polymer samples were used. The results presented here are for an isotactic PP, obtained via Ziegler-Natta catalysis, supplied by Borialis (Sines, Portugal), with a melt flow rate (MFR) = 38 g/10 min. The sample mass used was 12.761 mg. Pressed crimped 30-μl aluminum pans were used. The thermal lag resulting from the individual sample characteristics was measured by the procedure described below.

As shown by Richardson [10], the thermal lag due to the individual sample characteristics is symmetrical for heating and cooling scans, and it increases with the scanning rate. Also, the sample's thermal resistance changes with the scanning rate, from 25.112°/W at 8°C/min to 43.341°/W at 32°C/min (for the PP sample). The PP thermal resistance, measured at the indium melting temperature, is the difference between the reciprocal of the ascending slopes of two indium peaks, one with the standard calibration sample alone and another with the calibration sample in close contact, at the top of the polymer sample [6,11,12]. If a proper description of the crystallization process is to be achieved, this thermal resistance must also be duly taken into account.

RESULTS

The true onsets of the N → I transition (on heating), calculated from the measured values according to Eq. 10, and those for the I → N transition (on cooling), calculated according to Eq. 15, are shown in Fig. 1. On heating, the deviation of the onsets for the lowest and highest scanning rates used (respectively, 1°C/min and 32°C/min) is about 0.46°C (line 2 in Fig. 1); for cooling scans, the deviation is about 0.21°C (line 1 in Fig. 1). For scanning rates from 8°C/min up to 32°C/min, the difference between the onsets on heating and cooling, at the same scanning rate, is small (≤0.1°C), but slightly larger differences are obtained at lower cooling rates.

The supercooling of the liquid crystal was measured by extrapolating the corrected onsets, on heating and on cooling, to the zero scanning rate, and the value found was about 0.15°C. (One reviewer considers it surprising that this liquid crystal shows supercooling. The measured supercooling of this liquid crystal is small [0.15°C]. Values like this, or even higher [0.4°C], do exist in liquid crystalline transitions [see Ref. 13]. Possi-

MARCEL DEKKER, INC.
270 Madison Avenue, New York, New York 10016

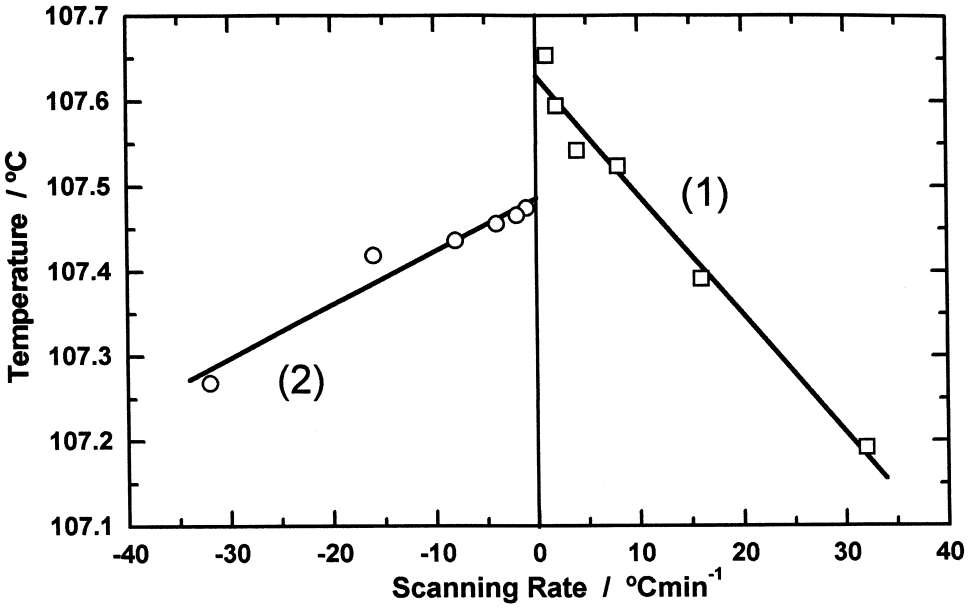

FIG. 1. (1) Onsets of the nematic to isotropic transition of CBOOA with calibration according to [10]. (2) Onset of the isotropic to nematic transition of CBOOA with the calibration on cooling according to [15].

bly, less supercooling could be obtained by purifying the liquid crystal. The supercooling then obtained may fall within the precision of differential scanning calorimeters [±0.1°C].) The deviations observed are thus acceptable within the experimental errors. On the other hand, if the results on cooling were obtained with the standard DSC heating calibration, the deviation between the onsets for $I \rightarrow N$ would be as large as 4°C, and therefore unacceptable, considering the relatively low supercooling associated with this transition. Probably, more accurate results could have been obtained if the other two corrections on cooling had been performed (the linear variation of the isothermal correction in the temperature range of interest and the thermal lag due to the sample's thermal resistance). (To establish the validity of the procedure for the calibration on cooling, one reviewer suggested the comparison with indium traces. The comparison was established and published [6]. Further, comparison with results obtained with a cooling calibration method developed by Menczel and Leslie [8] was also published in the same reference. The magnitude of the errors obtained with this calibration procedure is comparable to those obtained by Menczel and Leslie.) Other effects related to the kinetics of the $N \rightarrow I$ transition on heating, and the reverse on cooling, may also be responsible for the slopes of lines 1 and 2 in Fig. 1, in addition to that of the sample's purity. However, as referred to above, since the deviations are small, experimental errors related to the measurements may obscure a possible physical interpretation of those slopes.

The temperature at which the start of the PP sample's crystallization is detected depends on the cooling rate, as physically expected. For cooling rates of −1°C/min, the start of the crystallization is detected at 150°C, while at −32°C/min, it appears at 126°C. The supercooling at which regime transitions occur are 48°C for regime $I \rightarrow II$ and 60°C

MARCEL DEKKER, INC.
270 Madison Avenue, New York, New York 10016

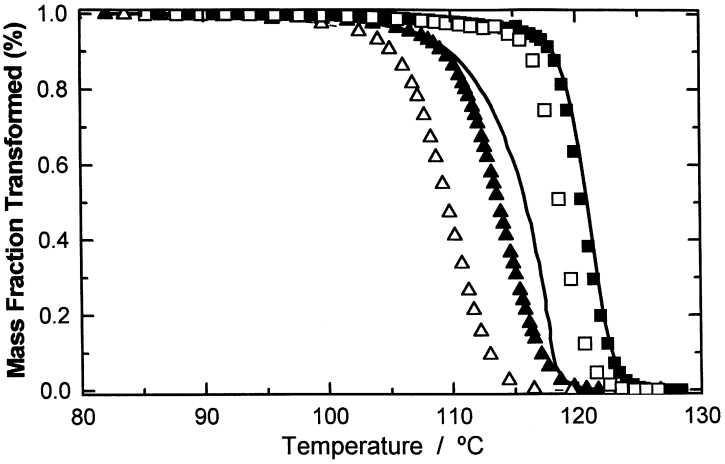

FIG. 2. Mass fraction transformed X versus temperature for nonisothermal crystallization of a PP (MFR 38 g/10 min) at the cooling rates ■ −8°C/min and ▲ −32°C/min. Open symbols are results obtained with the standard DSC calibration (Eq. 10), while solid symbols stand for results obtained with the calibration on cooling (Eq. 15); solid lines include the effect of the sample's thermal resistance as a function of the scanning rate.

for regime II → III [14]. Nonisothermal crystallization at −1°C/min develops within regime I; for cooling rates faster than −4°C/min, all the crystallization develops within regime III.

The thermodynamic melting temperature, obtained by the extrapolation plot of Hoffman and Weeks, was 186°C. This value agrees well with that obtained by Bu et al.,

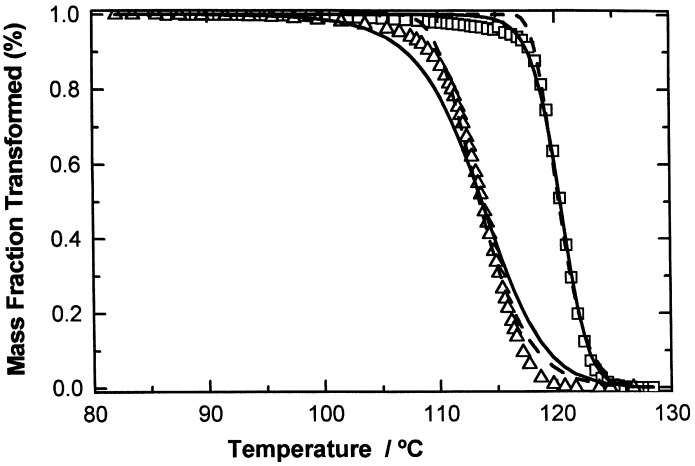

FIG. 3. Nonisothermal crystallization at the scanning rates □ −8°C/min and △ −32°C/min (results of calibration according to Eq. 15). Dashed line is the fit obtained with Namakura's equation. Solid line is the fit obtained with the Tobin-type nonisothermal equation.

MARCEL DEKKER, INC.
270 Madison Avenue, New York, New York 10016

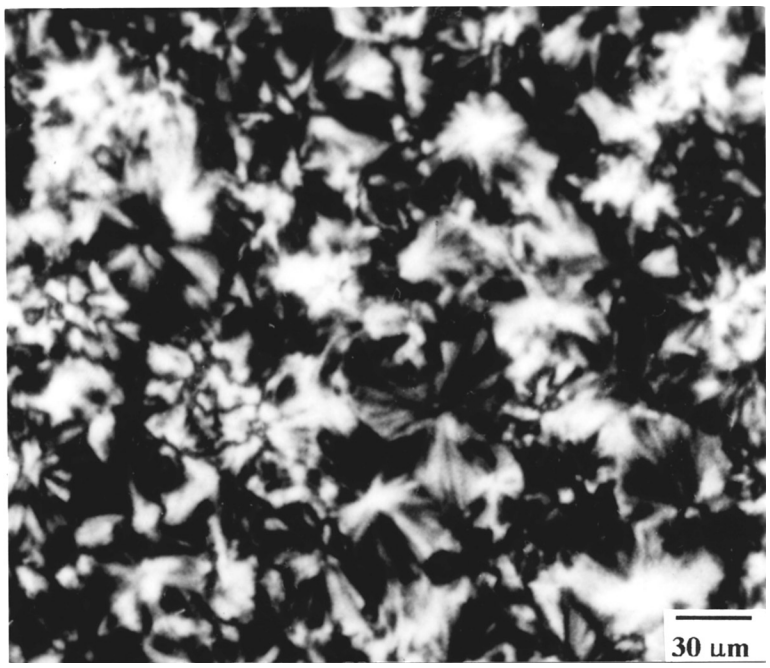

FIG. 4. Section of polypropylene crystallized in DSC at a scanning rate of −8°C/min.

187.4°C [15]. The glass transition temperature, measured in a DSC at a scanning rate of 10°C/min after a cooling run at the same rate, was −10°C. Using the value of $\Delta H_f^0 =$ 207.1 J/g [15], the degree of crystallinity changed from 48% for the material crystallized at −1°C/min to 44% for the material crystallized at −32°C/min. The transport term in the linear growth rate expression $G(T)$ of Eq. 6 was assumed to have a Williams, Landel, and Ferry (WLF) functionality, with $C_1 = 25$ and $C_2 = 30$ [17].

The growth rate of spherulites was measured during the isothermal crystallization in the hot stage of a polarized light optical microscope. The K_g parameter [$K_g = cb\sigma\sigma_e T_m^0/(k_b \Delta H)$, where c is 4 for regimes I and III and 2 for regime II, with the other parameters having their usual meaning] was obtained from a nonlinear fit of the linear growth rate equation to their measured values at each temperature. A great dispersion of values of K_g may be found in the literature, yielding σ_e values between 4×10^{-6} J/cm^{-2} and 1.2×10^{-5} J/cm^{-2} [17,18]. The value obtained for K_g yields a σ_e value of 1.6×10^{-5} J/cm^{-2} (with $b = 0.626$ nm, $\sigma = 1.1 \times 10^{-6}$ J/cm^2 and 0.936 g/cm^3 for the density of the α form), assuming that the crystallization developed in regimes I and III, which was verified for all scanning rates used (with the exception of the experiment at −2°C/min, which developed within regime II).

Open symbols in Fig. 2 show the results obtained with the standard DSC calibration (on heating) at the scanning rates of −8°C/min and −32°C/min. The effect of the calibration on cooling is shown by the solid symbols. At lower scanning rates, the shift is small, but it increases with the rate used. In practice, the effect of the calibration on cooling is to shift the curves obtained to higher temperatures, as if the experiment were

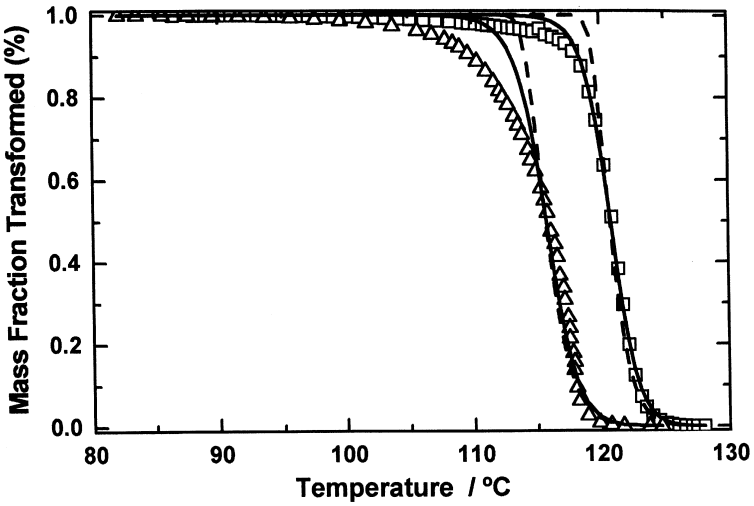

FIG. 5. Nonisothermal crystallization at the scanning rates of □ −8°C/min and △ −32°C/min. The experimental data are corrected for both the calibration on cooling and the change of the sample's thermal resistance with the cooling rate. Dashed line is the fit obtained with Namakura's equation. Solid line is the fit obtained with the Tobin-type nonisothermal equation.

performed with the standard DSC calibration at a lower scanning rate. For example, the kinetics for −16°C/min (not shown in the figure), with the calibration according to Eq. 15, is similar to the one obtained with the standard calibration at −8°C/min.

For modeling purposes, using a minimum set of parameters, the use of an accurate temperature scale is important, especially if some of the physical parameters involved are obtained from isothermal experiments, for which the experiments can be performed with an accurate temperature scale. Figure 3 shows the description of the nonisothermal crystallization process, at the scanning rates indicated, with the Nakamura and Tobin-type nonisothermal equations, Eqs. 5 and 9, respectively. The experimental data have been corrected for the calibration on cooling according to Eq. 15, and an athermal nucleation has been assumed.

The Avrami (or Tobin exponent) was fixed exactly at 3, which is a very severe constriction. The only varying parameter was the overall preexponential factor, which includes the shape factor of the growing semicrystalline structures, the ratio between the solid and liquid phase densities, the mean number of active nuclei, and the preexponential factor of the linear growth rate, some of which are most difficult to predict or measure with any degree of confidence.

Experimental support for $n = 3$ was supplied by microscopic observation of the boundaries between the spherulites of samples crystallized in a DSC at scanning rates from −1°C/min to −32°C/min. Figure 4 shows a section of a sample crystallized in a DSC at −8°C/min as viewed by polarized optical microscopy. Although the dimensions of the spherulites are small, it may be seen that the spherulite boundaries are straight lines. Also, at the scanning rates used in this work, only α spherulites were formed. Even in sections of samples cooled from the melt into ice, only α spherulites were observed. Transcrystalline layers did appear, as expected, at the top and bottom of the sample, and

a reduced number of cornrow structures were formed. Since the exponent n is an average value for the dimension of the crystalline structures, it may be concluded that, on average, spherulitic structures are created, and that they are activated almost at the same time, at the start of the crystallization process.

A better description of the crystallization process may possibly be achieved if an additional correction is performed. In fact, if the variation of the particular sample's thermal resistance with the scanning rate is included in Eq. 16, the resulting change of the real sample temperature and the ensuing crystallization kinetics are those shown in Fig. 5. This figure also shows the description of the crystallization process with the two model equations considered above. As may be seen, from comparison with the data in Fig. 3, a better description of the crystallization process is achieved in the latter case. The agreement may certainly still be improved, after a more elaborate data treatment procedure, by which the true sample temperature scan rate (directly resulting from Eq. 16) is used in the equations of $X(T)$ instead of the instrument-controlled one. By interpolating or extrapolating the values obtained for the only varying parameter, quantitative predictions of the nonisothermal crystallization process kinetics may therefore be achieved for intermediate or higher scanning rates (below the supercooling at which the formation of α spherulites becomes important).

CONCLUSIONS

The error associated with the method used for the DSC calibration on cooling is small (less than 0.5°C) for scanning rates up to 32°C/min. The deviation between the results obtained with the standard DSC calibration and those obtained with a calibration on cooling increased with the cooling rate. A proper temperature calibration is imperative at high cooling rates—both the calibration on cooling as such and the correction for the sample's thermal resistance and its change with the scanning rate. The fits obtained by Eqs. 5 and 9 over the results of Fig. 5 are similar (sum of least squares $\approx 10^{-2}$, $n \approx 3$). Results obtained from data with the standard DSC calibration yield poor fits, as well as values of n other than 3, which is the expected value for athermal nucleation. Additional differences between the behavior predicted and the experimental data may be due to the probable existence, at the scanning rates used, of some degree of thermal nucleation, as well as the possible occurrence of primary and secondary crystallization processes, in addition to possible small errors in the actual sample temperature scan rates. These, however, will require more elaborate modeling.

ACKNOWLEDGMENT

We thank Borialis for supplying the material used in this work and Dr. Jovita Oliveira for the photograph of Fig. 4.

REFERENCES

1. K. Nakamura, T. Watanabe, K. Katayama, and T. Amano, *J. Appl. Polym. Sci.*, *16*, 1077 (1972).
2. J. A. Martins and J. J. C. Cruz Pinto, *Polymer*, *41*, 6875 (2000).
3. J. A. Martins and J. J. C. Cruz Pinto, unpublished, 1996.
4. T. Ozawa, *Polymer*, *12*, 150 (1971).

5. C. N. Velisaris and J. C. Seferis, *Polym. Eng. Sci.*, *24*, 1402 (1988).
6. J. A. Martins and J. J. C. Cruz Pinto, *Thermochim. Acta*, *332*, 179 (1999).
7. M. J. Richardson and N. G. Savil, *Thermochim. Acta*, *12*, 213 (1975).
8. J. D. Menczel and T. M. Leslie, *J. Thermal Anal.*, *40*, 957 (1993).
9. B. Wunderlich, *Macromolecular Physics*, Vol. 2, Academic, New York, 1976.
10. M. J. Richardson, *Thermochim. Acta*, *300*, 15 (1997).
11. V. A. Bershtein and V. M. Egorov, *Differential Scanning Calorimetry of Polymers*, Ellis Horwood Series in Polymer Science and Technology, Chichester, England, 1994.
12. J. H. Flynn and D. M. Levin, *Thermochim. Acta*, *126*, 93 (1988).
13. N. Oranth and F. Strhbusch, *Ber. Bunsenges. Phys. Chem.*, *91*, 211 (1987).
14. J. Varga, Crystallization, melting and supermolecular structure of isotactic polypropylene, in *Polypropylene: Structure*, *Blends and Composites*, *Vol. 1: Structure and Morphology* (J. Karger-Kocsis, Ed.), Chapman and Hall, Cambridge, England, 1995, chap. 3.
15. H. S. Bu, S. Z. D. Cheng, and B. Wunderlich, *Makromol. Chem. Rapid Commun.*, *9*, 76 (1988).
16. R. L. Miller (Ed.), *Flow Induced Crystallization in Polymer Systems*, Gordon and Breach Science Publishers, 1977.
17. B. Monasse and J. M. Haudin, *Colloid Polym. Sci.*, *263*, 822 (1985).
18. A. Galeski, Nucleation in polypropylene, in *Polypropylene: Structure*, *Blends and Composites*, *Vol. 1: Structure and Morphology* (J. Karger-Kocsis, Ed.), Chapman and Hall, Cambridge, England, 1995, chap. 4.

Received July 16, 1999
Revised March 4, 2000
Accepted March 6, 2000